International Journal of the Korean Society of Precision Engineering, Vol. 2, No. 2, July 2001.

Measurement Error Modeling for On-Machine Measurement of Sculptured Surfaces

Myeong-Woo Cho[1], Se-Hee Lee[1] and Tae-Il Seo[2]

[1] School of mechanical engineering, Inha University, Incheon, Korea
[2] Center for Integrated Technology Assistance for Die & Molds, KITECH, Incheon, Korea

ABSTRACT

The objective of this research is to develop a measurement error model for sculptured surfaces in On-Machine-Measurement (OMM) process based on a closed-loop configuration. The geometric error model of each axis of a vertical CNC machining center is derived using a 4×4 homogeneous transformation matrix. The ideal locations of a touch-type probe for the sculptured surface measurement are calculated from the parametric surface representation and X-, Y-directional geometric errors of the machine. Also, the actual coordinates of the probe are calculated by considering the pre-travel variation of a probe and Z-directional geometric errors. Then, the step-by-step measurement error analysis method is suggested based on a closed-loop configuration of the machining center including workpiece and probe errors. The simulation study shows the simplicity and effectiveness of the proposed error modeling strategy.

Keywords : On-Machine-Measurement, Sculptured Surface, Geometric Errors, Pre-travel variation, Measurement Errors

1. Introduction

Generally, sculptured surfaces are machined on the CNC machine tools according to the predefined sequence (from rough cut to finish cut), and finishing processes are followed. After finishing all the machining processes, the machined workpieces are moved on the inspection instruments, such as CMM(Coordinate Measuring Machine), for dimensional measurement. The computer controlled CMM plays an important role as a measuring station for precise and complicated surface shapes by applying Computer-Aided Inspection techniques[1,2,3]. However, since the CMMs can generally be used only for the measurement of finished products, it is not easy to measure the shape accuracy of a workpiece during machining process on the machine tools. Since almost of the important dimensions of the workpieces are determined during the machining processes using machine tools, it would be time consuming to know whether the workpieces are out of tolerances or not in the CMM process. In order to improve these drawbacks, the OMM (On-Machine-Measurement) techniques have been studied[4,5,6] recently. The OMM systems use a sensing probe, instead of tools, to measure the dimensional accuracy of workpieces on the machine. Since the machining and inspection processes can be preformed in one machine, the OMM method can simplify the inspection process without moving a workpiece to the CMM. Also, after checking the dimensions, required and/or modified machining process can be followed to increase the accuracy of the machined surface. However, since the accuracy of the machine tool is generally worse than that of the CMM, the OMM method cannot give good measurement results comparing with the CMM.

Machine tool errors can be categorized as quasi-static errors and dynamic errors[7,8]. The main sources of dynamic errors are machine tool vibration, chatter, and spindle vibration. Quasi-static errors are mainly due to the geometric inaccuracy of the machine, caused by the influence of static loading, and thermal effects on the machine structure. Among the quasi-static errors, the geometric error of a machine is one of the major error sources contributing to the inaccuracy of the OMM system.

In the OMM process, touch trigger probes are most widely used to obtain the geometric information of the surface. In using a touch trigger probe, there is an idle moving distance, called "*pre-travel*", until the probe generates an electric signal after contacting the surface[10]. Such various error sources cause the inaccuracies of the *measurement results using OMM system. In this study, a* measurement error modeling method for sculptured surfaces in OMM process is suggested based on the closed-loop configuration[9] by integrating machine geometric errors, probing errors and workpiece geometric representations. To achieve the objective of this research, the geometric error components of a vertical type three-axis CNC machining center are described as 4×4 homogeneous transformation matrices. Also, the probe pre-travel errors are represented as matrix form to derive the integrated error model. To validate the proposed approaches, simulation works are carried out.

2. Geometric Error Modeling of a Machine Tool

As shown in the Fig.1, a vertical CNC machining center is composed of three linear moving carriages, **X**- and **Y**-directional moving table for workpiece and **Z**-axis for vertical movement of rotating tool. When a linear carriage moves, there can be six error terms, three *translational and three rotational errors*, caused by the degree of freedom of rigid body motion. Among the three translational errors, one error term is the positioning error defined by the difference between the actual carriage position and the scale reading, and the other two errors are called the straightness errors measured along the axis perpendicular to the carriage moving direction. The three rotational angles are called roll, pitch, and yaw with respect to the carriage moving direction. When two or more linear axes are combined, other geometric parameters must be introduced to specify the angular orientation of the axis with respect to each other. This is called the squareness error, which is caused by geometric relationships between the axes.

2.1 Translational and rotational errors

The *translational and rotational errors of motion* along the **X**-axis are shown in Fig. 1. The geometric error components of three-axis can be denoted as follows:

$\mathbf{EX_i(X_j)}$: $\mathbf{X_i}$-directional component of translational errors when moving along $\mathbf{X_j}$-axis

$\mathbf{EA_i(X_j)}$: $\mathbf{X_i}$-directional component of rotational errors when moving along $\mathbf{X_j}$-axis

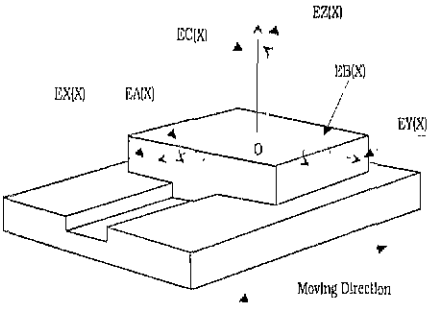

Fig. 1 Error components in **X**-directional movement

If the rotational terms are very small, then the following approximation can be derived by considering only first-order error terms along the **X**-axis.

$$T_i = \begin{bmatrix} 1 & -EC(X) & EB(X) & EX(X)+Dx \\ EC(X) & 1 & -EA(X) & EY(X) \\ EB(X) & EA(X) & 1 & EZ(X) \\ 0 & 0 & 0 & 1 \end{bmatrix} \quad (1)$$

Here, $\mathbf{T_i}$ represents the transformation matrix with respect to the origin of the machine coordinate, and **Dx** *represents the X-directional position. The subscript* ***i*** represents the **X**-axis carriage movement. Similarly, the representation of the translational and rotational errors of motion along the **Y**-axis, denoted as $\mathbf{T_j}$, and **Z**-axis, denoted as $\mathbf{T_k}$, can be determined.

2.2 Squareness errors

If **Z** is set to be the reference axis, one is the squareness error between the **X**- and **Z**-axis, the other is the error between the **Y**- and **Z**-axis, which can be denoted as follows:

$\mathbf{EA_i(XZ)}$: $\mathbf{X_i}$-directional component of the squareness error between X- and Z-axis

$\mathbf{EA_i(YZ)}$: $\mathbf{X_i}$-directional component of the squareness error between Y- and Z-axis

If the squareness errors are assumed to be very small, the errors between **X**- and **Z**-axis can be approximated as

follow:

$$T_{ik}=\begin{bmatrix} 1 & -EC(XZ) & EB(XZ) & 0 \\ EC(XZ) & 1 & 0 & 0 \\ EB(XZ) & 0 & 1 & 0 \\ 0 & 0 & 0 & 1 \end{bmatrix} \quad (2)$$

Similarly, the squareness error terms between Y-and Z-axis, denoted as T_{jk}, can be determined.

2.3 Geometric errors caused by carriage movement

The transformation matrix at the desired position due to the motion along the X-axis (T_x) can be obtained by adding the squareness errors at the desired point and the translational and rotational errors of the X-axis through the following steps.

When the carriage moves along the X-axis by Dx, the matrix form of the position can be represented as

$$L_x=\begin{bmatrix} 1 & 0 & 0 & Dx \\ 0 & 1 & 0 & 0 \\ 0 & 0 & 1 & 0 \\ 0 & 0 & 0 & 1 \end{bmatrix} \quad (3)$$

Then, the error component at the desired point due to the squareness errors between the X- and Z-axes is obtained as follows:

$$T_{xz} = T_{ik} L_x - L_x$$

$$=\begin{bmatrix} 0 & -EC(XZ) & EB(XZ) & 0 \\ EC(XZ) & 0 & 0 & EC(XZ)Dx \\ EB(XZ) & 0 & 0 & -EB(XZ)Dx \\ 0 & 0 & 0 & 0 \end{bmatrix} \quad (4)$$

The translational and rotational errors along the X-axis can be described based on Eq.(1).

$$T_x = T_1 + T_{xz}$$

$$=\begin{bmatrix} 1 & (T_x)_{12} & (T_x)_{13} & (T_x)_{14} \\ (T_x)_{21} & 1 & (T_x)_{23} & (T_x)_{24} \\ 0 & (T_y)_{32} & 1 & (T_x)_{34} \\ 0 & 0 & 0 & 1 \end{bmatrix} \quad (5)$$

where $(T_x)_{12} = -EC(X)-EC(XZ)$
$(T_x)_{13} = EB(X)+EB(XZ)$
$(T_x)_{14} = EX(X)+Dx$
$(T_x)_{21} = EC(X)+EC(XZ)$
$(T_x)_{23} = -EA(X)$
$(T_y)_{24} = EY(X)+EC(XZ)Dx$
$(T_x)_{32} = EA(X)$
$(T_x)_{34} = \mathbf{EZ(X)-EB(XZ)Dx}$

Similarly, the transformation matrix due to motion along the Y-axis (T_y) and Z-axis (T_z) can be determined.

3. Probe Error Modeling

The most widely being used sensor types in OMM process are touch trigger probes. In the measurement process, the probe approaches to the surface until it touches the object. After touching the surface, the probe continues to move to reach a threshold setting for triggering a signal. The idle moving distance between the touch instant and the trigger instant is called as probe pre-travel, which accounts for the majority of touch trigger probe errors and is mainly caused by bending deflection of the stylus shaft[10]. The pre-travel errors are highly repeatable errors according to the probe approaching direction. Since the pre-travel error is one of the main errors in OMM process, this error term should be included in the error modeling procedure.

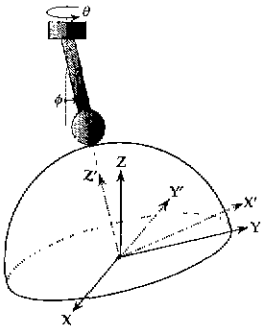

Fig. 2 Probe coordinate system

3.1 Probe coordinate

Since the probe pre-travel errors are varying with the surface normal vectors, it would be convenient to introduce a coordinate system, which is called the probe coordinate as shown in Fig.2. In the figure, (x', y', z') denotes the probe coordinates, and (x, y, z) denotes the machine coordinates. Here, ϕ and θ represent tilt and roll angle between two coordinate frames. If two coordinate

frames have common origins, the relationship between two frames can be represented as follows:

$$[x'\ y'\ z'\ 1]^T = T_P\,[x\ y\ z\ 1]^T \qquad (6)$$

where, ($\mathbf{T_P}$) is a 4×4 coordinate transformation matrix between two coordinate frames.

3.2 Probe pre-travel error

The probe pre-travel errors, vary with the probing direction, can be measured and compensated using master ball as shown in Fig. 3. Here, $\mathbf{R_e}$ denotes the effective radius of a probe ball, $\mathbf{PE}(\phi_i,\theta_j)$ denotes the probing error defined along (ϕ_i,θ_j) direction of the master ball. $\mathbf{R_s}(\phi_i,\theta_j)$ represents the radius of the master ball at (ϕ_i,θ_j), and $\mathbf{R_m}(\phi_i,\theta_j)$ represents the distance between the master ball and probe ball centers respectively. Then, the following relationship can be obtained.

$$\mathbf{R_e} - \mathbf{PE}(\phi_i,\theta_j) = \mathbf{R_m}(\phi_i,\theta_j) - \mathbf{R_S}(\phi_i,\theta_j) \qquad (7)$$

Here, for more effective error compensation, the effective radius of the probe is used instead of the nominal radius of the probe as shown in Fig.3. Since $\mathbf{R_m}(\phi_i,\theta_j)$ and $\mathbf{R_s}(\phi_i,\theta_j)$ are given values, the effective radius $\mathbf{R_e}$ can be obtained from the constant terms and the probing error $\mathbf{PE}(\phi_i,\theta_j)$ can be obtained from the varaible terms of the right-hand side terms in Eq.(7).

Thus, in the OMM process, the probing directions are determined as the normal vector of the surface. If the unit normal vector, which represents the probing direction defined in the machine coordinate frame, is denoted as ($\mathbf{M_x}$, $\mathbf{M_y}$, $\mathbf{M_z}$), the transformation matrix **TL** due to the probing error can be obtained as follows:

$$\mathbf{TL} = \mathbf{PE}(\phi_i,\theta_j)\,[M_x\ M_y\ M_z\ 1]^T \qquad (8)$$

If the components $\mathbf{N_x}$, $\mathbf{N_y}$, $\mathbf{N_z}$ of surface normal vector are given, ϕ and θ can be calculated as follows:

$$\phi = \cos^{-1} N_z\ ,\ \theta = \tan^{-1}\left(\frac{N_y}{N_x}\right) \qquad (9)$$

4. Error Analysis Based on the Closed Loop Configuration

In this study, a measurement error analysis method for sculptured surfaces using OMM is suggested based on the closed-loop configuration by integrating machine geometric errors, probing errors, and sculptured surface representations. This research results can be used effectively for the measurement error compensation in the OMM process for sculptured surfaces.

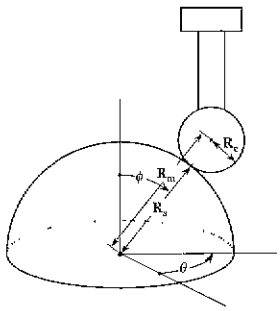

Fig. 3 Probe error calibration

4.1 Closed-loop configuration

The measurement error at the final probing point can be obtained by calculating the difference between the positioning point on the workpiece and the probe position. Thus, the following equation can be obtained from the Fig.4.

$$\mathbf{X} + \mathbf{Y} + \mathbf{W} = \mathbf{Z} + \mathbf{P} \qquad (10)$$

where **X**, **Y** and **Z** represent movements along each axis, **W** represents a distance between the machine origin and the measuring point on the surface and **P** represents the location of probe contact point.

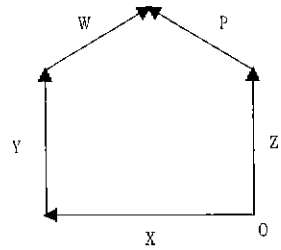

Fig. 4 Closed-loop configuration for the multi-axis machine tool (ideal case)

However, due to the volumetric error, Eq.(10) does not hold. Therefore, the volumetric error will be denoted by the difference between the carriage error of the table

and the probe as illustrated in Fig.5.

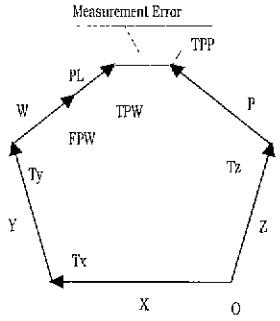

Fig. 5 Closed-loop configuration for the multi-axis machine tool (including errors)

4.2 Calculation of probe location

If there does not exist any errors when measuring a sculptured surface, the ideal location of probe can be determined by considering the probe diameter and a unit normal vector on the measuring point. For a Bezier parametric surface, the measuring point **W** on this surface can be represented as follows:

$$\mathbf{W} = [\ W_x \quad W_y \quad W_z \quad 1\ ]^T$$

$$= r(u,v) = \sum_{i=0}^{m} \sum_{j=0}^{n} P_{ij} \bullet B_{i,m}(u)\, B_{j,n}(v) \quad u,v \in [0,1] \tag{11}$$

where $\mathbf{P}_{ij}$ are the vertices of the control polyhedron, $\mathbf{B}_{i,m}(v)$ are the Bernstein polynomials.

Required coordinate of the probe ball center **PL** for the given measuring point can be obtained as follows:

$$\mathbf{PL} = [\ P_x \quad P_y \quad P_z \quad 1\ ]^T = \mathbf{W} + R\,\mathbf{N} \tag{12}$$

where PL is the theoretical coordinate of probe ball center described by ($\mathbf{PL}_x$, $\mathbf{PL}_y$, $\mathbf{PL}_z$), R is nominal radius of probe ball, **W** represents the coordinate of measuring point determined by Eq.(11), and **N** represents the corresponding unit normal vector.

4.3 Measurement errors based on closed-loop configuration

Based on the difference between the coordinates of ideal and actual porbe positions, the measuring errors of the OMM system can be modeled as follows.

4.3.1 Ideal location of probe ball center

Tihe transformation matrix on the moving table can be obtained as follows:

$$\mathbf{T}_{xy} = \mathbf{T}_x \mathbf{T}_y \tag{13}$$

where, $\mathbf{T}_{xy}$ represents the transformation matrix with respect to the origin of the reference frame when **X**- and **Y**-directional movements exist.

The matrix representation of the workpiece surface with **X**- and **Y**-directional movement can be described by the matrices product of $\mathbf{T}_x$, $\mathbf{T}_y$ and **W**, which is represented as follows:

$$\mathbf{FPW} = \mathbf{T}_x \mathbf{T}_y \mathbf{W} = \begin{bmatrix} \mathbf{FPX(W)} \\ \mathbf{FPY(W)} \\ \mathbf{FPZ(W)} \\ 1 \end{bmatrix} \tag{14}$$

where, **W** indicates a 3-dimensional workpiece position. Row 1, 2 and 3 in the matrix **FPW** represents the actual location of measuring point taking into account the measuring errors.

The ideal location of probe ball corresponding to a given measuring point can be determined by Eq.(12) and, as shown in Eq.(14), the actual location can be represented as follows:

$$\mathbf{TPW} = \begin{bmatrix} \mathbf{TPX(W)} \\ \mathbf{TPY(W)} \\ \mathbf{TPZ(W)} \\ 1 \end{bmatrix} = \mathbf{PL} = \begin{bmatrix} \mathbf{FPX(W)} + \mathbf{RN}_x \\ \mathbf{TPY(W)} + \mathbf{RN}_y \\ \mathbf{TPZ(W)} + \mathbf{RN}_z \\ 1 \end{bmatrix} \tag{15}$$

4.3.2 Actual location of the measuring points

When using a vertical machining center, the probe moves along **Z**-axis. Thus, to determine the measuring errors, the **Z**-directional geometric error components and dircetion-dependant pre-travel variations should be combined. If **TPP** represenetes the coordinate transformation of probe ball center with respect to the machine coordinate, this can be determined as follows:

$$\mathbf{TPP} = \mathbf{T}_z \mathbf{TL} = \begin{bmatrix} \mathbf{TPX(T)} \\ \mathbf{TPY(T)} \\ \mathbf{TPZ(T)} \\ 1 \end{bmatrix} \tag{16}$$

where $\mathbf{T}_z$ is a 4×4 transformation matrix representing

the geometric error components and **TL** is probing errors given by Eq.(8).

4.3.3 Determination of measuring errors

Finally, 3-dimensional measuring errors of the OMM system can be determined from Eq.(15) and Eq.(16) as follows:

$$VE = TPW - TPP = \begin{bmatrix} TPX(W) \\ TPY(W) \\ TPZ(W) \end{bmatrix} - \begin{bmatrix} TPX(T) \\ TPY(T) \\ TPZ(T) \end{bmatrix} = \begin{bmatrix} VEX \\ VEY \\ VEZ \end{bmatrix} \quad (17)$$

where **VEX**, **VEY** and **VEZ** represent **X**-, **Y**- and **Z**-directional measuring error components. Therefore, the overall measuring error amount can be determined as follows:

$$\| VE \| = \sqrt{(VEX)^2 + (VEY)^2 + (VEZ)^2} \quad (18)$$

5. Simulation Study

In this paper, when carring out the OMM process for sculptured surfaces on a vertical CNC machining center, a measurement error model was proposed by integrating the geometric of machining center and the probing errors. To validate the efficiency of the proposed approach, following simulation works were established.

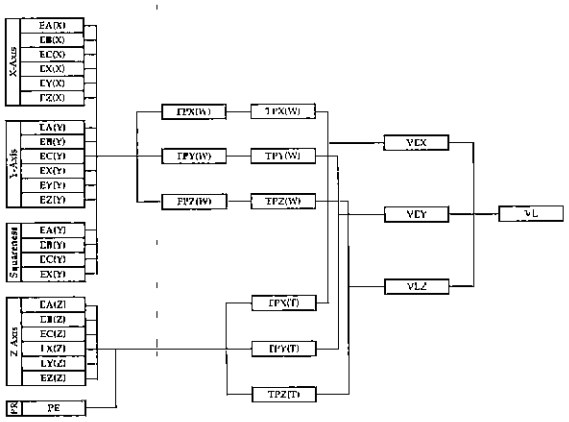

Fig. 6 Error components in OMM process using vertical machining center

5.1 Error components

Fig. 6 shows the geometric error components of the OMM system using a vertical CNC machining center. Fig. 7 shows translational and rotational errors for each axis used in the simulation works. The moving range of carriage table corresponds to 1000mm along each axis and each error component was defined as 0 at the machine origin. Then, the values of each error component were generated in the in the interval of 50mm. Table 1 shows squareness errors of **X**- and **Y**-axes with respect to **Z**-axis.

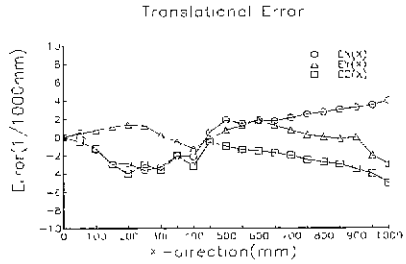

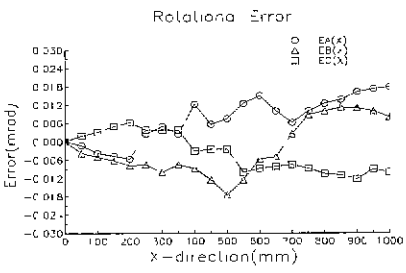

(a) X-directional error components

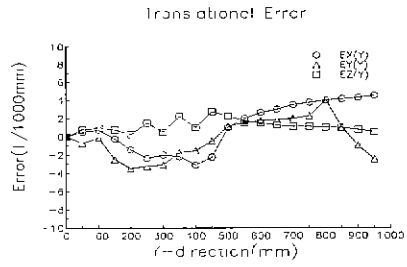

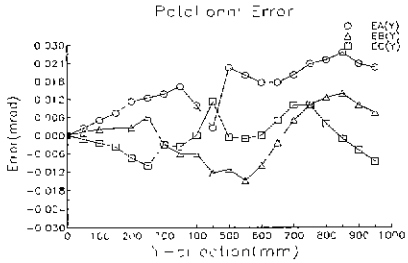

(b) Y-directional error components

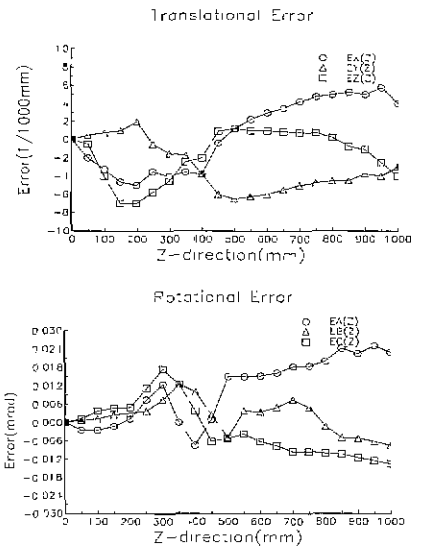

(c) Z-directional error components

Fig. 7 Error components of a machine tool

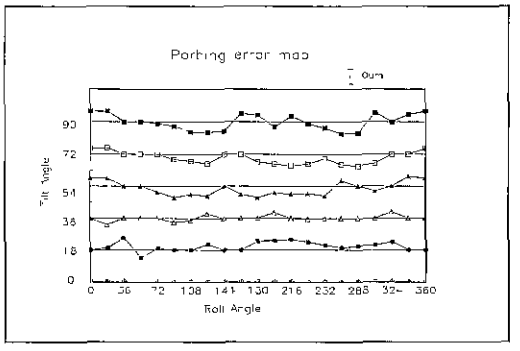

Fig. 8 Pre-travel error of a touch-type probe

The probing errors are represented by functions of tilt angle ϕ and roll angle θ according to the probe approaching direction. When using the OMM system on a vertical CNC machining center, the range of tilt angle ϕ corresponds to from 0° to 90° and the range of roll angle θ corresponds to from 0° to 360°. In the simulation works, the tilt angle ϕ was divided in 5 increments and the roll angle θ was divided in 20 increments. In this case, the probing errors generated as shown in Fig. 8.

Table 1 Squareness errors

Between X and Z	Between Y and Z
EA(XZ) = 0.067 mrad	**EA(YZ)** = 0.026 mrad
EB(XZ) = 0.010 mrad	**EC(YZ)** = 0.021 mrad

5.2 Simulation

When the OMM system being used on a vertical CNC machining center, the target surface was fixed on the carriage table moving along **X**- and **Y**-axes. Therefore, the geometric errors induced by the table movement can be represented by a calculation of transformation matrices as shown in Eq.(18).

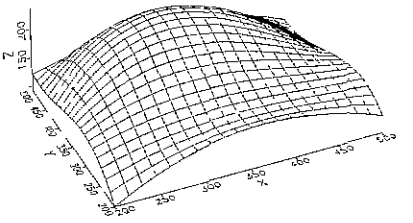

Fig. 9 Sculptured surface workpiece

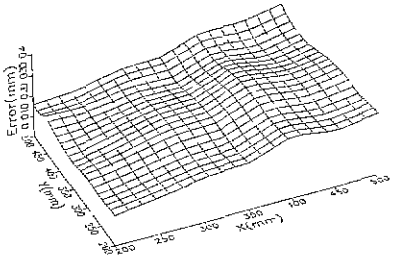

(a) Measurement errors caused by geometric errors of a 3-axis machine tool

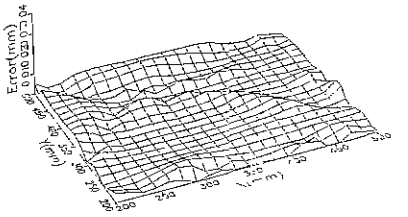

(b) Measurement errors caused by probe pre-travel errors

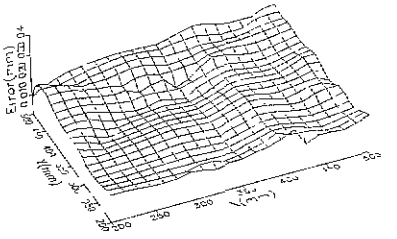

(c) Integrated measurement errors by proposed method

Fig. 10 Measurement errors for a sculptured surface

By applying the proposed approach, obtained simulation results are illustrated in Fig. 10. Fig. 10-(a) shows the simulation results considering only the geometric erros of the machining center, Fig. 10-(b) shows the simulation results considering only the probing errors and Fig. 10-(c) shows the results combined these two errors. These results, in fact, were obtained without considering the thermal errors of the machining center, the distortion errors induced by workpiece fixture, and so on. Thus, these simulation results may be somewhat different from the real case. However, the results of this study can show the possibilty of an integrated error modeling method when other error sources are included.

6. Conclusions

The objective of this study is to suggest a measurement error modeling method for OMM system vertical CNC machining center. Taking into account the geometric errors of the machining center and the probing errors, the measurement errors can be predicted and the integrated mesurement errors were obtained through the simulation works. The conclusions of this study can be summarized as follows:

(1) When using the OMM system on the vertical machining center, the measurement errors were modeled based on the closed loop configuration.
(2) Combining the gemetric errors of the machining center, the coordinate transformation of the target measuring points and the probing errors, the effective error modeling method was proposed.
(3) Through homogeneous trasnformation matrices, it was possible to more simply and easily determine the measurement errors.
(4) To validate the proposed approach, the simulation works were carried out and final measurement errors were obtained.
(5) It is possible to develop an improved model taking into account other error sources, for example, thermal errors of the machining center.

References

1. Pahk, H. J., Kim, W. D., and Ahn, W. J., "Development of Precision Inspection Technique for Aircraft Parts Having Very Thin Features Based on CAD/CAI Integration," Journal of KSME, Vol. 20, No. 6, pp. 1743-1752, 1996.
2. Cho, M. W. Kim, M. K., and Kim, K., "Flexible Inspection System Based on a Vision Guided Coordinate Measuring Machine," International Journal of Production Research, Vol. 33. No. 5, pp. 1433-1448, 1995.
3. Duffie, N., Bollinger, J., and Kronenberg, M., "CAD Directed Inspection and Error Analysis Using Patch Database," Annals of the CIRP, Vol. 33, pp. 347-350, 1984.
4. Nam, W. S., and Chung, S. C., "Development of On-the-Machine Measurement and Inspection System for Freeform Surfaces," Proceedings of KSPE Autumn Conference. pp. 911-914, 1997.
5. Lee, S. J., Kim, S. H., and Kim, O. H, "On-Machine-Measurement System Scanning Probe Point to Point Measurement," Proceedings of KSPE Conference in Spring, pp. 73-77, 1997.
6. Mou. J.. and Richard Liu, C., "A Method for Enhancing the Accuracy of CNC Machine Tools for On-Machine Inspection," Journal of Manufacturing Systems, Vol. 11. No. 4, pp. 229-236. 1992.
7. Ferreira, P. M., and Richard Liu, C., "A Method for Estimating and Compensating Quasi-static Errors of Machine Tools," Journal of Engineering for Industry. Vol. 115, Feb., 1993.
8. Chatterjee, S.. "An Assessment of Quasi-Static and Operational Errors in NC Machine Tools." Journal of Manufacturing Systems, Vol. 16. No. 1. pp. 59-68, 1997.
9. Cho, J. H. Cho, M. W., and Kim, K. "Volumetric Error Analysis of a Multi-axis Machine Tool Machining a Sculptured Surface Workpiece," International Journal of Production Research, Vol. 32. No. 2, pp. 345-363, 1994.
10. Shen. Y.. and Moon. S., "Mapping of Probe Pre-travel in Dimensional Measurements Using Neural Networks Computational Technique," Computers in Industry, Vol. 34. pp. 295-306. 1997.